Efficient and broadband polarization rotator using horizontal slot waveguide for silicon photonics

Huijuan Zhang,[1,a)] Suchandrima Das,[2,3] Ying Huang,[1] Chao Li,[1] Shiyi Chen,[1] Haifeng Zhou,[1] Mingbin Yu,[1] Patrick Guo-Qiang Lo,[1] and John T. L. Thong[2,b)]
[1]*Institute of Microelectronics, A*STAR (Agency for Science, Technology and Research), 11 Science Park Road, Science Park II, 117685 Singapore*
[2]*Department of Electrical and Computer Engineering, National University of Singapore, 117576 Singapore*
[3]*Advanced Micro Devices Singapore, 469032, Singapore*

(Received 5 June 2012; accepted 21 June 2012; published online 10 July 2012)

We report an efficient and low-loss polarization rotator based on mode evolution using horizontal slot waveguide. The device is fabricated using complementary metal–oxide–semiconductor compatible processes, which allows monolithic integration with active drive electronics and other photonic components. A rotator fabricated with 100 μm transition length provides a high extinction ratio >14 dB for both transverse-magnetic (TM)-transverse-electric (TE) and TE-TM rotation. The excess loss of the device is <1 dB for both rotations as etching of the bottom Si waveguide is prevented. The device also exhibits a uniform rotation response over C+L band wavelength range of 1530-1600 nm. © *2012 American Institute of Physics*. [http://dx.doi.org/10.1063/1.4734640]

Silicon (Si) photonics has received much attention in recent years for its ability to integrate electronic and optical components on the same silicon chip.[1,2] Process compatibility with complementary metal–oxide–semiconductor (CMOS) technology makes the mass production of Si photonics devices cost-effective. The high index contrast of Si-on-insulator (SOI) allows for ultra-compact photonic circuits with small footprint.[3,4] Modulators,[5,6] photodetectors,[7,8] filters,[9,10] switches,[11,12] and other passive devices[13,14] based on Si waveguides have been demonstrated. However, this high-index contrast in SOI waveguides leads to a polarization-dependent wavelength shift and phase shift. As this polarization sensitivity is undesirable, in order to circumvent the problem, several polarization diversity circuits have been reported.[15–17] A polarization rotator then becomes a key element in the polarization diversity circuit in order to achieve a single polarization state in the photonic circuit. Several mode-evolution based polarization rotators have been proposed.[18–23] However, a few of aforementioned reports only consist of simulation work without experimental demonstration or demonstrate functional devices that are not Si-based.[4,19,21,23] The silicon wire based polarization rotator has either limited extinction ratio (~11 dB)[18] or is intrinsically difficult for integration with other SOI photonic devices.[20] In the latter work, a high extinction ratio (~15 dB) was reported for transverse-electric (TE) mode to transverse-magnetic (TM) mode rotation, but the extinction ratio is only ~8 dB for TM-TE rotation, accompanied by a high (5~6 dB) insertion loss. The low TM-TE rotation efficiency was attributed to the etched top surface of waveguides in the transition region introducing additional loss, which may degrade the rotation performance. Moreover, partial etching of the Si waveguide presents a process control challenge as under- or over-etching would lead to performance degradation. In addition, it is rather difficult to integrate germanium (Ge)-on-Si photodetector with this device as epitaxial growth of Ge on Si has strict requirements of a pristine Si surface.[24] The specially designed Si waveguide thickness (200 nm) may also require extra effort when it comes to integrating other functional devices that are dimension-sensitive, such as splitters, directional couplers, and ring resonators.

Here, we report a polarization rotator based on mode evolution and phase matching between a horizontal slot waveguide and a channel waveguide. A low index material, namely silicon oxide (SiO_2) here, is inserted between high index Si layers so as to confine light in the slot region.[25] The proposed device containing a horizontal slot waveguide for the rotation region has high process robustness and can be readily integrated with other SOI photonic components. Compared to our previous work,[17,20] the key point of adding a slot layer is to avoid the partial etching in the Si channel waveguide so as to reduce the insertion loss and improve the performance of the device. The presence of a slot layer is also very helpful in process control, as discussed below. A mode size converter is included in the device to connect the slot waveguide to the channel waveguide so as to reduce potential loss arising from mode mismatch. In the current design, the proposed rotator using a horizontal slot waveguide can be readily implemented in a polarization diversity circuit. The performance of the device is evaluated through experiments.

A schematic of the polarization rotator is shown in Fig. 1. The device consists of four parts: (i) an input channel waveguide, (ii) a mode size converter to couple the light from a channel waveguide to a horizontal slot waveguide, (iii) a horizontal slot waveguide, (iv) an asymmetric tapered structure as the polarization transition region, and (v) an output channel waveguide. Initially, light with TM polarization as illustrated propagates in a channel waveguide (Fig. 1(i)). The light is guided into a horizontal slot waveguide by an adiabatic mode size converter (Fig. 1(ii)). The transition region for efficient and low loss mode conversion is designed to have a symmetric inverted lateral taper. This taper structure gradually pulls out the field and guides it into the horizontal

a)Electronic mail: zhangh@ime.a-star.edu.sg.
b)Electronic mail: elettl@nus.edu.sg.

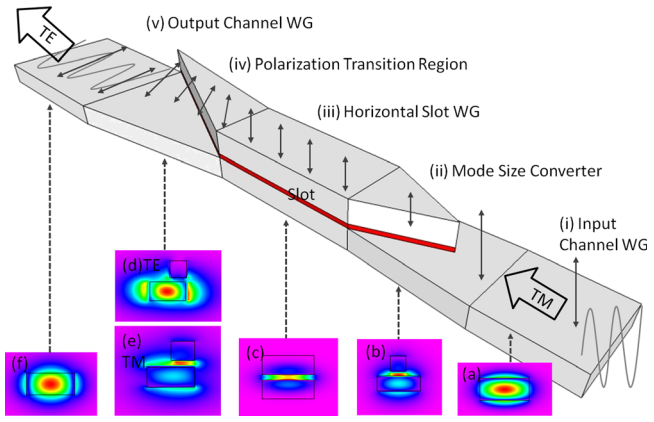

FIG. 1. Schematic of the polarization rotator consisting of input waveguide, mode size converter, horizontal slot waveguide, polarization transition region, and final output channel waveguide. Insets (a)–(f) are mode profiles along the device when launching TM, respectively. The mode profiles are obtained through 3D-FDTD simulation using RSOFT at 1550 nm wavelength. WG stands for waveguide.

slot region. After propagation in the horizontal slot waveguide (Fig. 1(iii)) for mode stabilization, the fundamental TM mode interacts with an asymmetric taper structure to one side of the waveguide (Fig. 1(iv)) to gradually rotate the light into TE mode. While this rotation occurs, the slot waveguide slowly transforms back to a channel waveguide as the output (Fig. 1(v)). These transformations have negligible intrinsic loss as mode evolution occurs rather than coupling between modes. The double arrows in Fig. 1 indicate the evolution of quasi-electric field along the light propagation. Finite-difference time-domain (FDTD) simulations were carried out to evaluate the device performance using RSOFT. The mode profiles ((a)–(f)) in Fig. 1 are shown at various locations along the proposed device to illustrate the mode evolution. It is observed that the input TM mode is completely rotated by the proposed device into TE mode and vice versa.

To verify the concept, we designed the device based on following parameters: the top and bottom Si layers of the proposed device have a thickness of 250 nm while the SiO_2 slot has a thickness of 60 nm. The bottom and upper cladding is 2 μm SiO_2. To achieve the best rotation result, phase matching condition should be satisfied for the TM-carrying horizontal slot waveguide (Fig. 1(iv)) and the TE-carrying output channel waveguide (Fig. 1(v)).[18] The effective indices of the input TM slot and the output TE channel waveguide are calculated using RSOFT for varying waveguide widths (w_s for slot and w_c for channel waveguide, respectively) at the operating wavelength 1550 nm (Fig. 2(a)). The phase matching condition is found to be satisfied when $w_s = 240$ nm and $w_c = 320$ nm, so that $n_{eff}(TM_{in}) = n_{eff}(TE_{out})$ while taking into consideration the ease of fabrication. The chosen width also satisfies the phase matching condition for $n_{eff}(TE_{in}) = n_{eff}(TM_{out})$. Therefore, the device is expected to achieve both TM-to-TE and TE-to-TM rotation when TM or TE is launched into the input channel waveguide. One could vary the Si thickness depending the device application and photonic circuit design and adjust the waveguide width accordingly to satisfy the phase matching condition.

Devices were fabricated on an 8-in. Si wafer with a 2 μm SiO_2 layer. The process starts with a multilayer deposition using plasma enhance chemical vapor deposition (PECVD): 250 nm amorphous Si as the bottom Si layer followed by 60 nm SiO_2 as the slot and finally 250 nm amorphous Si as the top Si layer. The bottom layer could be crystalline Si if a SOI wafer is used. Next, waveguide structures were patterned by optical lithography using a 248 nm Nikon scanner. The wafer was then etched using reactive ion etching (RIE) to the bottom Si surface. A second layer of optical lithography was carried out to protect the horizontal slot waveguide region and expose the channel waveguide region (Fig. 2(b)). Another round of RIE was performed to etch the bottom Si layer and also part of the top Si layer at the transition region. In this process, the slot waveguide serves as an etch-stop layer for the bottom Si layer in the second RIE (Fig. 2(c)), with a etch selectivity of 1:7 in our RIE system. Hence, the fabrication process here is easily controlled and slight over-etching was introduced to completely remove the top Si at desired location without significantly attacking the bottom Si waveguide. The critical parameters of the polarization rotator, namely the thickness of the top and bottom Si layers, are ensured by controlling the thickness of the film deposition. Therefore, these dimensions are highly repeatable. The process presented here is more favorable than that for the Si waveguide based rotator as dimension control for the latter is highly dependent on the two-step etching (partial etching) of the same Si material.[17,20,21] Any under- or over-

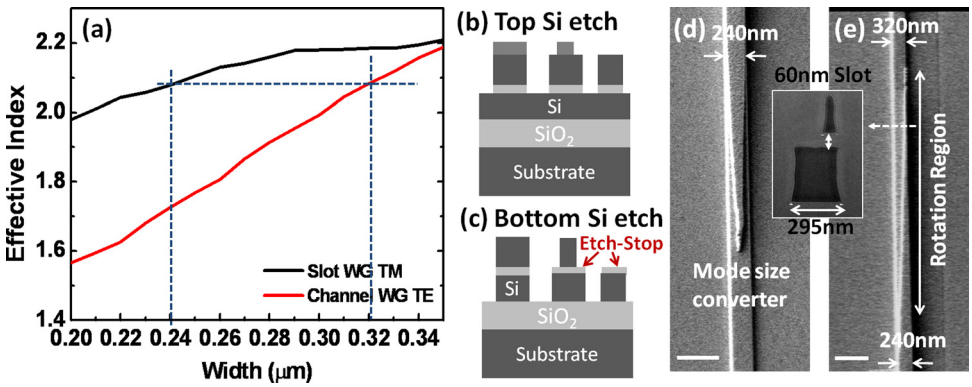

FIG. 2. (a) Effective indices of the fundamental TE and TM modes of a SiO_2 cladding slot waveguide (black line) and channel waveguide (red line) with different widths, respectively. Dashed lines indicated the chosen parameters satisfying the phase matching condition. Schematic of the key process steps (b) after top Si layer etching and (c) after bottom Si layer etching. The slot layer acted as an etch-stop layer to eliminate possible attack of the bottom Si. SEM images of (d) the mode size converter and (e) the polarization rotation region. Scale bars: 500 nm. Inset is a TEM image of the cross section at the indicated position.

etching leads to undesired variation from the design parameters. The lateral dimensions of the rotator (i.e., widths) are defined by lithography, which is well-controlled. Fig. 2(d) shows a scanning electron microscope (SEM) image of the mode size converter having transition length of 5 μm in the fabricated device connecting the channel waveguide (bottom) and the horizontal slot waveguide (top). Fig. 2(e) shows the polarization transition region having length of 10 μm between the horizontal waveguide (bottom) and the channel waveguide (top). The inset is a transmission electron microscopy (TEM) image of the cross section of the polarization transition region in the rotator indicated by the dashed arrow. The inspection point is chosen along the device to demonstrate the gradual change of the structure. The slot thickness is indicated as 60 nm between the top and bottom Si layers. The width of the bottom Si at the inspection point is around 295 nm. It is observed that the bottom Si surface remains unetched because of the slot protection.

The device performance was first characterized using a tunable laser source at 1550 nm. Polarization of the light was controlled by a polarization controller, and polarization maintaining (PM) fibers were used throughout the tests. Light was coupled into waveguide through an inverted taper structure with a tip size of 180 nm.[26] The light was then guided into a horizontal slot waveguide, propagated through the mode size converter, and gradually transformed into its orthogonal mode by the tapered rotating region. The output light was then coupled back into a PM fiber. At the output fiber end, a second polarizer was connected to measure the power of TE and TM components separately to examine the polarization rotation performance of the device. Measurements were done under both TE and TM launch conditions. The transition lengths of the rotators varied from 10 to 500 μm. Fig. 3(a) shows the polarization extinction ratios of the rotators, which is defined as $10\log\left(\frac{Ex_o^2}{Ey_o^2}\right)$ for TM-TE rotation and $10\log\left(\frac{Ey_o^2}{Ex_o^2}\right)$ for TE-TM rotation. We observed polarization rotation in all the measurements using the fabricated device for different rotating length. In general, the extinction ratio increases with the transition length as observed in Fig. 3(a). The increase in extinction ratio is not strictly proportional to the increase in the transition length as complete rotation will occur beyond a certain transition length; in our case, 100 μm is sufficient, beyond which the extinction ratio stabilizes. Efficient rotations of 14.15 dB for TM-to-TE rotation and 14.50 dB for TE-to-TM rotation were achieved by a 100 μm rotation device. For rotating lengths less than 100 μm, it is noted that the extinction ratio for TM-TE is generally lower than for TE-TM. This is attributed to the highly confined TM mode in the horizontal slot waveguide, which leads to more efficient rotation of the TE mode for a short rotating region compared with non-confined TE-TM rotation. This observation confirms the benefit of inserting a slot into the rotator. For the Si waveguide based rotator, the TM-TE rotation requires a longer transition length than needed for TE-TM rotation. In addition, beyond the saturating rotation length, almost complete rotation occurs for both TE-TM and TM-TE rotation. The rotation length required ($\sim$100 μm) of the slot waveguide based rotator is considerably shorter than the previously reported Si_3N_4-on-Si rotator (420 μm)[22] and Si_3N_4 rotator (600 μm).[15] Fukuda *et al.* reported a double-core rotator with a short rotation length ($\sim$35 μm) that has a lower TE-TM extinction ratio (11 dB).[16] The device has an even lower TM-TE rotation performance ($<$10 dB) with a relatively narrow band response.

To characterize the broadband response, the polarization rotators were also tested from 1530 to 1600 nm using an amplified spontaneous emission (ASE) source and an optical spectrum analyzer (OSA). All of the fabricated devices demonstrated broadband polarization rotation. Figs. 3(b)

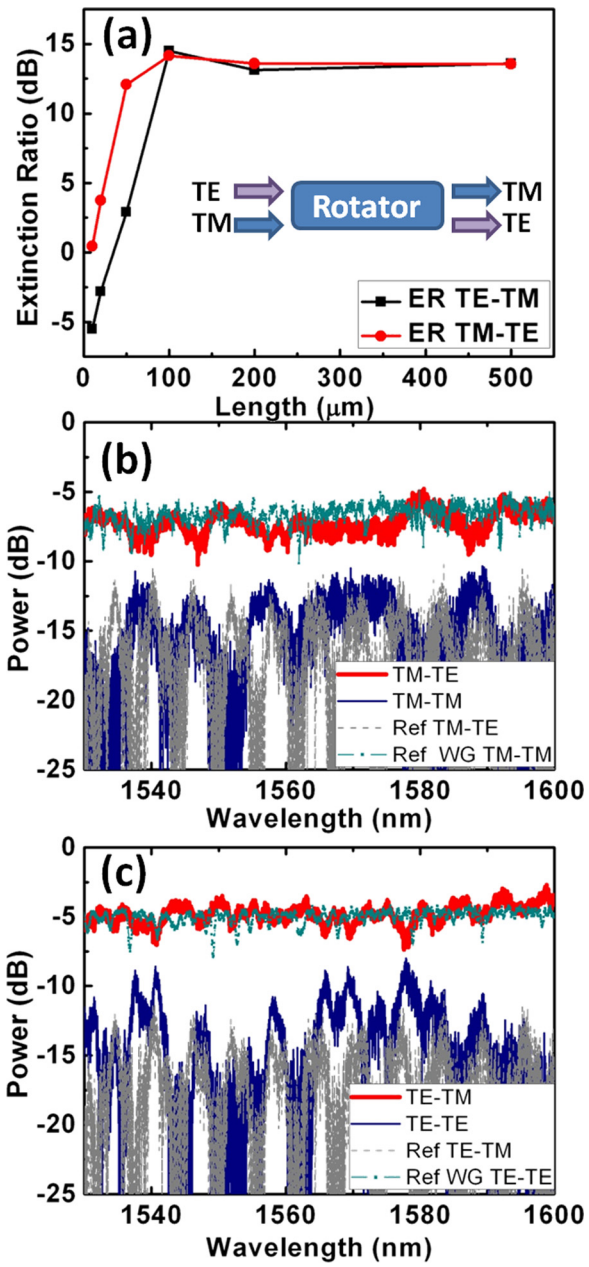

FIG. 3. (a) Extinction ratio of devices with various rotating length from 10 to 500 μm. Both TM and TE launching conditions were tested and output TM-TE rotation (red dot) and TE-TM rotation (black square) were measured. Input light wavelength is 1550 nm. (b) Measured polarization components when launching TM. TE is red line and remained TM is blue line. Dashed and dashed dotted lines are background noise TM-TE and reference Si waveguide TM-TM. (c) Measured polarization components when launching TE. TM is red line and remained TE is blue line. Dashed and dashed dotted lines are background noise TE-TM and reference Si waveguide TE-TE. The scanning wavelength is 1530 to 1600 nm.

and 3(c) show the measured polarization components from a polarization rotator with a 100 μm transition length when launching TM and TE, respectively. The output spectra were recorded using an OSA. Our polarization rotator has an almost flat response from 1530 to 1600 nm with small fluctuations. Reference data for a straight waveguide on the same chip with TM-TM and TE-TE power and background noise for TM-TE and TE-TM are included in Figs. 3(b) and 3(c). It is observed that the excess loss from the fabricated rotator is less than 1 dB by comparing the output power from the rotator and the reference waveguide. Test waveguides were included in the device chip to investigate individual loss contributions. The coupling loss from fiber to waveguide is ~2 dB per facet and the propagation loss of the waveguide is 5.20 dB/cm for TE mode and 2.38 dB/cm for TM mode. The insertion loss from the mode size converter is about 0.5 dB for both TE and TM mode. Hence, the excess loss for the rotation region is only 0.5 dB and may be considered nearly lossless due to the long gradual field transformation during the mode evolution. The low-loss and broadband response of the rotator makes it an ideal device for real implementation for telecommunications applications.

In summary, an efficient and broadband polarization rotator with low insertion loss is reported in this Letter. The introduction of a slot in the polarization rotating region enables better process control and provides high extinction ratios >14 dB for both TM-TE and TE-TM rotations. The device is compact in footprint and readily fabricated using CMOS-compatible processes. The proposed device also brings about an additional benefit of easy integration with Si photonics platform, especially with Ge-on-Si photodetectors. The polarization rotator is readily implemented in a polarization diversity circuit.

[1]T. Tsuchizawa, K. Yamada, H. Fukuda, T. Watanabe, J. Takahashi, M. Takahashi, T. Shoji, E. Tamechika, S. Itabashi, and H. Morita, IEEE J. Sel. Top. Quantum Electron. **11**, 232 (2005).
[2]D. A. B. Miller, IEEE J. Sel. Top. Quantum Electron. **6**, 1312 (2000).
[3]S. Nakamura, T. Chu, M. Ishizaka, M. Tokushima, Y. Urino, M. Sakauchi, I. Nishioka, and K. Fukuchi, in *Proceedings of ECOC* (2008), p. 175.
[4]F. Xia, L. Sekaric, and Y. Vlasov, Nat. Photonics **1**, 65 (2007).
[5]A. Liu, R. Jones, L. Liao, D. Samara-Rubio, D. Rubin, O. Cohen, R. Nicolaescu, and M. Paniccia, Nature (London) **427**, 615 (2004).
[6]Q. Xu, S. Manipatruni, B. Schmidt, J. Shakya, and M. Lipson, Opt. Express **15**, 430(2007).
[7]T.-Y. Liow, K.-W. Ang, Q. Fang, J.-F. Song, Y.-Z. Xiong, M.-B. Yu, and G.-Q. Lo, IEEE J. Sel. Top. Quantum Electron. **16**, 307–315 (2010).
[8]L. Chen, P. Dong, and M. Lipson, Opt. Express **16**, 11513 (2008).
[9]P. Dong, W. Qian, H. Liang, R. Shafiiha, X. Wang, D. Feng, G. Li, J. E. Cunningham, A. V. Krishnamoorthy, and M. Asghari, Opt. Express **18**, 24504 (2010).
[10]M. S. Rasras, D. M. Gill, M. P. Earnshaw, C. R. Doerr, J. S. Weiner, C. A. Bolle, and Y.-K. Chen, IEEE Photon. Technol. Lett. **22**, 112 (2010).
[11]Y. Shoji, K. Kintaka, S. Suda, H. Kawashima, T. Hasama, and H. Ishikawa, Opt. Express **18**, 9071 (2010).
[12]M. Yang, W. M. J. Green, S. Assefa, J. Van Campenhout, B. G. Lee, C. V. Jahnes, F. E. Doany, C. L. Schow, J. A. Kash, and Y. A. Vlasov, Opt. Express **19**, 47 (2010).
[13]H. Yamada, T. Chu, S. Ishida, and Y. Arakawa, IEEE Photon. Technol. Lett. **17**, 585–587 (2005).
[14]B. Guha, B. B. C. Kyotoku, and M. Lipson, Opt. Express **18**, 3487 (2010).
[15]T. Barwicz, M. R. Watts, M. A. Popovic, P. T. Rakich, L. Socci, F. X. Kartner, E. P. Ippen, and Henry. I. Smith, Nat. Photonics **1**, 57 (2007).
[16]H. Fukuda, K. Yamada, T. Tsuchizawa, T. Watanabe, H. Shinojima, and S. Itabashi, Opt. Express **16**, 4872 (2008).
[17]J. Zhang, H. Zhang, S. Chen, M. Yu, G. Q. Lo, and D. L. Kwong, Opt. Express **19**, 13063 (2011).
[18]H. Fukuda, K. Yamada, T. Tsuchizawa, T. Watanabe, H. Shinojima, and S. Itabashi, Opt. Express **16**, 2628 (2008).
[19]M. R. Watts and H. A. Haus, Opt. Lett. **30**, 138 (2005).
[20]J. Zhang, M. Yu, G.-Q. Lo, and D.-L. Kwong, IEEE J. Sel. Top. Quantum Electron. **16**, 53 (2010).
[21]Z. Wang and D. Dai, J. Opt. Soc. Am. B **25**, 747 (2008).
[22]L. Chen, C. R. Doerr, and Y.-K. Chen, Opt. Lett. **36**, 469 (2011).
[23]N.-N. Feng, R. Sun, J. Michel, and L. C. Kimerling, Opt. Lett. **32**, 2131 (2007).
[24]C. Li, H. Zhang, S. Chen, J. Zhang, N. Duan, M. Yu, and G.-Q. Lo, IEEE Photon. Technol. Lett. **24**, 781 (2012).
[25]V. R. Almeida, Q. Xu, C. A. Barrios, and M. Lipson, Opt. Lett. **29**, 1209 (2004).
[26]V. R. Almeida, R. R. Panepucci, and M. Lipson, Opt. Lett. **28**, 1302 (2003).